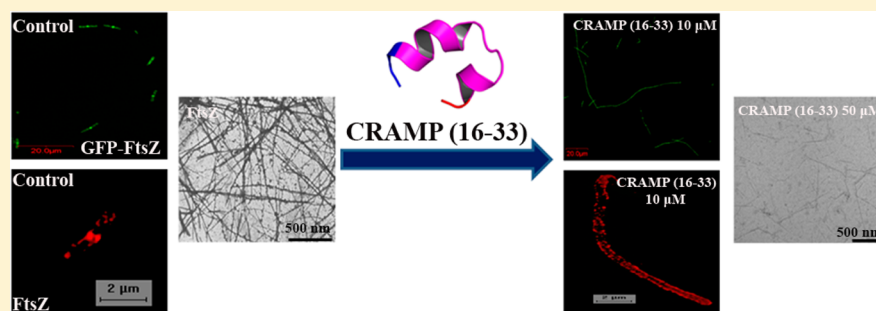


Antimicrobial Peptide CRAMP (16–33) Stalls Bacterial Cytokinesis by Inhibiting FtsZ Assembly

Shashikant Ray, Hemendra Pal Singh Dhaked, and Dulal Panda*

Department of Biosciences and Bioengineering, IIT Bombay, Powai, Mumbai 400076, India

S Supporting Information



ABSTRACT: A cathelin-related antimicrobial peptide (CRAMP) of 37 amino acid residues is thought to regulate innate immunity and provide a host defense mechanism in mammals. Here, a part of the CRAMP peptide, CRAMP (16–33) (GEKLKKIGQKIKNFFQKL), was found to bind to FtsZ and to inhibit the assembly and GTPase activity of FtsZ *in vitro*. A computational analysis indicated that CRAMP (16–33) binds in the cavity of the T7 loop of FtsZ. Both hydrophobic and ionic interactions were involved in the binding interactions. Further, CRAMP (16–33) inhibited the formation of the FtsZ ring in bacteria, indicating that it inhibited bacterial cell division by inhibiting FtsZ assembly.

A cathelin-related antimicrobial peptide (CRAMP) was found in multicellular organisms and reported to provide innate immunity to fight against microbes.¹ It is mainly expressed in neutrophil granules^{2,3} and sites exposed to various microbes like the first line of defense system, skin, and gastrointestinal tract.⁴ CRAMP inhibits the growth of several pathogenic bacteria in the gut of mouse.⁵ The secondary structure of CRAMP shows an amphipathic α -helical conformation like other antimicrobial peptides.^{3,6} It was thought that it causes bacterial cell death by cell membrane permeabilization because of the amphipathic α -helical conformation.³ CRAMP induces elongation of bacterial cells, indicating that it inhibits bacterial cytokinesis.⁵ The active part of CRAMP, i.e., CRAMP (16–33) (GEKLKKIGQKIKNFFQKL), was also found to inhibit the growth of several bacterial species such as *Escherichia coli*, *Bacillus subtilis*, *Staphylococcus aureus*, *Streptococcus pyogenes*, *Salmonella typhimurium*, and *Pseudomonas aeruginosa*.⁷ CRAMP (16–33) is a cationic peptide with an overall charge of 4.8 at pH 7.4. Further, CRAMP (16–33) displays a sequence that is partially similar to that of the C-terminus of MclZ, a 40-amino acid protein that is known to inhibit FtsZ assembly.⁸ Therefore, we examined the effect of CRAMP (16–33) on the assembly of FtsZ *in vitro* as well as *in vivo*. As reported previously,⁷ CRAMP (16–33) was found to inhibit the proliferation of *B. subtilis* and *E. coli* cells. For example, 10 and 20 μ M CRAMP (16–33) inhibited the growth of *B. subtilis* by 78 ± 5 and 100%, respectively, with respect to the control. Further, 40 and 50 μ M CRAMP (16–

33) inhibited the proliferation of *E. coli* cells by 73 ± 8 and 100%, respectively, with respect to the control. CRAMP (16–33) treatment increased the mean length of *B. subtilis* cells. The average length of *B. subtilis* cells was estimated to be 3.8 ± 4 and $18 \pm 8 \mu$ m in control and 10 μ M CRAMP (16–33)-treated cells, respectively, suggesting that CRAMP (16–33) inhibited bacterial cytokinesis. A perturbation of the assembly of FtsZ is known to cause bacterial cell length elongation and to inhibit bacterial cytokinesis.^{9,10}

The localization of the FtsZ ring (Z-ring) at the mid cell position was monitored using either a GFP-FtsZ construct in *B. subtilis* 2020 cells¹¹ or indirect immunostaining in *B. subtilis* 168 cells using a monoclonal antibody of FtsZ. In control cells, FtsZ was localized at the mid cells and proper Z-rings were observed (Figure 1A,B). When the *B. subtilis* 2020 cells and wild-type *B. subtilis* 168 cells were grown in the presence of 10 μ M CRAMP (16–33), most of the treated cells were found to be elongated and FtsZ was either diffused throughout the cells or localized in the form of incomplete septa (Figure 1A,B). For example, 63% of the *B. subtilis* 168 cells had Z-rings at the mid cell position, whereas 25% of the 10 μ M CRAMP (16–33)-treated cells contained Z-rings.

Because CRAMP (16–33) induced cell elongation and perturbed Z-ring formation in bacteria, we examined its effect

Received: September 3, 2014

Revised: October 7, 2014

Published: October 7, 2014

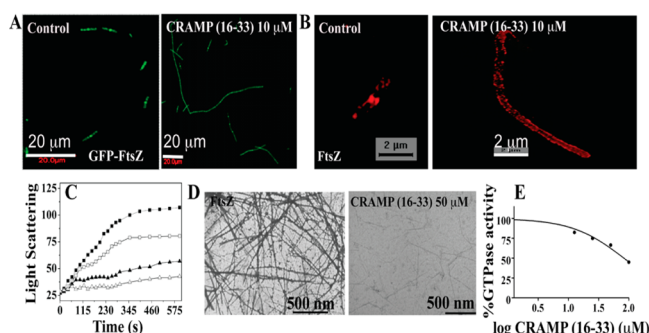


Figure 1. CRAMP (16–33) perturbed the assembly of FtsZ both *in vivo* and *in vitro*. CRAMP (16–33) (10 μ M) inhibited Z-ring formation in (A) *B. subtilis* 2020 and (B) *B. subtilis* 168 cells. (A) The Z-ring in *B. subtilis* 2020 cells was visualized by expressing GFP-FtsZ, and the scale bar is 20 μ m. (B) FtsZ was visualized (red) using an antibody in *B. subtilis* 168 cells. The scale bar is 2 μ m. (C) Effect of CRAMP (16–33) on the assembly kinetics of FtsZ. FtsZ (6 μ M) was polymerized in 25 mM Pipes buffer (pH 7.4), 5 mM MgCl₂, and 50 mM KCl containing 1 mM GTP in the (■) absence or presence of (□) 50, (▲) 100, and (△) 150 μ M CRAMP (16–33) at 37 °C. (D) Effects of CRAMP (16–33) on the assembly of FtsZ were observed via electron microscopy. (E) CRAMP (16–33) reduced the GTPase activity of FtsZ.

on the assembly and GTPase activity of FtsZ *in vitro*. CRAMP (16–33) inhibited the assembly of FtsZ in a concentration-dependent manner. For example, as compared to the control, 50 and 150 μ M CRAMP (16–33) inhibited the assembly of FtsZ by 34 ± 6 and $80 \pm 2\%$, respectively (Figure 1C). Further, electron microscopy analysis showed fewer and finer polymers of FtsZ in the presence of 50 μ M CRAMP (16–33) compared to those with the control (Figure 1D), suggesting that CRAMP (16–33) inhibited the assembly and bundling of FtsZ polymers. However, under the condition used, CRAMP (16–33) did not have any noticeable effect on the assembly of purified tubulin (Figure S1 of the Supporting Information).

CRAMP (16–33) inhibited the GTPase activity of FtsZ in a concentration-dependent manner (Figure 1E). For example, 50 and 150 μ M CRAMP (16–33) suppressed the GTPase activity of FtsZ by 42 ± 8.5 and $64 \pm 11\%$, respectively, compared to the control. The half-maximal inhibitory concentration (IC₅₀) for the GTPase activity was determined to be 70 ± 14 μ M (Figure 1E). The GTPase activity of FtsZ may be reduced either due to the inhibition of GTP binding or due to a reduction in the level of hydrolysis of GTP. Therefore, the effect of CRAMP (16–33) on the binding of GTP to FtsZ was monitored using TNP-GTP, a fluorescent analogue of GTP^{12,13} (Figure S2A of the Supporting Information). Under the conditions used, 50 and 100 μ M CRAMP (16–33) did not inhibit the binding of TNP-GTP to FtsZ, indicating that it does not share its binding site on FtsZ with GTP. As reported previously,¹³ both GTP and MciZ were found to inhibit the binding of TNP-GTP to FtsZ (Figure S2A of the Supporting Information).

Because CRAMP (16–33) displays a sequence partially similar (39%) to that of the C-terminus of MciZ, the effect of CRAMP (16–33) on the binding of MciZ to FtsZ was monitored using fluorescently labeled MciZ. As observed previously,¹³ GTP inhibited the fluorescence intensity of the FITC-MciZ-FtsZ complex while 50 and 100 μ M CRAMP (16–33) had no effect on the binding of FITC-MciZ to FtsZ (Figure S2B of the Supporting Information). GTP (50 μ M) inhibited

the fluorescence intensity of the FITC-MciZ-FtsZ complex by $65 \pm 19\%$ compared to the control. The results indicated that CRAMP (16–33) does not share its binding site on FtsZ with GTP.

A docking study revealed that CRAMP (16–33) may bind in the cavity of the T7 loop of FtsZ (Figure 2A). Both

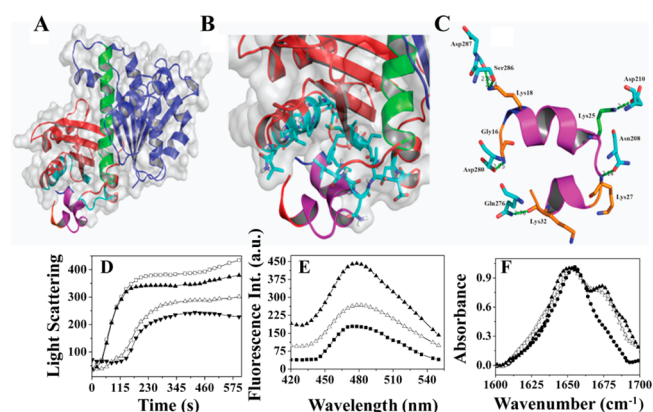


Figure 2. Binding interaction of CRAMP (16–33) and FtsZ. (A) Identification of a putative binding site for CRAMP (16–33) on FtsZ. The N-terminus, H7 helix, and C-terminus of FtsZ are colored blue, green, and red, respectively. CRAMP (16–33) is depicted as a magenta cartoon model. The N-terminus and C-terminus of CRAMP (16–33) are colored blue and red, respectively. (B) Magnified view of the binding cavity of CRAMP (16–33). The residues of FtsZ lying within 4 Å of CRAMP (16–33) are shown as sticks (cyan color). (C) Residues of CRAMP (16–33) involved in a salt bridge (green) and hydrogen bonding (orange) are shown as sticks. (D) FtsZ (6 μ M) was polymerized for 10 min in 25 mM Pipes buffer (pH 7.4), 5 mM MgCl₂, and 250 mM KCl containing 1 mM GTP in the (□) absence or presence of (▲) 50, (△) 100, and (▼) 150 μ M CRAMP (16–33). (E) Effects of CRAMP (16–33) on the ANS fluorescence in the presence of FtsZ. FtsZ (3 μ M) was incubated (■) without and with (△) 100 and (▲) 150 μ M CRAMP (16–33) in 25 mM Pipes buffer (pH 7.4) for 15 min on ice and then incubated with ANS for 30 min at 25 °C. The spectra were recorded using 360 nm as the excitation wavelength. Spectra of appropriate blanks were subtracted from their respective data sets. (F) Effects of CRAMP (16–33) on the secondary structures of FtsZ. FtsZ (10 μ M) was incubated without and with 100 and 150 μ M CRAMP (16–33) in 10 mM phosphate buffer (pH 6.8) at 25 °C for 15 min. FTIR spectra were recorded for (●) 10 μ M FtsZ and 10 μ M FtsZ with (△) 100 and (▲) 150 μ M CRAMP (16–33) using 0, 100, and 150 μ M CRAMP (16–33) in 10 mM phosphate buffer (pH 6.8) as a baseline.

hydrophobic and hydrophilic residues were found to be involved in the interaction of CRAMP (16–33) with FtsZ. Further, an analysis indicated that Leu206, Ile207, Asn208, Asp210, Asp213, Leu272, Val275, Gln276, Ala279, Asp280, Val282, Ala283, Ser284, Ser286, Asp287, Val290, Asn291, Met292, Ile293, and Phe294 residues of FtsZ were located within 4 Å of CRAMP (16–33) (Table S1 of the Supporting Information and Figure 2B). Moreover residues of the T7 loop of FtsZ that interacted with CRAMP (16–33) are Leu206, Ile207, Asn208, and Asp210 (bold in Table S1 of the Supporting Information). We observed that CRAMP (16–33) binding was stabilized through salt bridge, hydrogen bonding, hydrophilic, and hydrophobic interactions with FtsZ (Table S2 of the Supporting Information). Asp210 (located at the T7 loop of FtsZ) forms a salt bridge interaction with Lys25 of the CRAMP (16–33) peptide. CRAMP (16–33) residues Gly16, Lys27, and Lys32 form hydrogen bonds with Asp280,

Asn208, and Gln276 residues of FtsZ, respectively. The Lys18 residue of CRAMP (16–33) forms a H-bond with both Ser286 and Asp287 residues of FtsZ (Figure 2C).

In the presence of 50 mM KCl, 50, 100, and 150 μ M CRAMP (16–33) inhibited the polymerization of FtsZ by 34 ± 6 , 59 ± 4 , and $80 \pm 2\%$, respectively. However, in the presence of 250 mM KCl, 50, 100, and 150 μ M CRAMP (16–33) inhibited the polymerization by 15 ± 1.5 , 33 ± 4.5 , and $56 \pm 7\%$, respectively (Figure 2D), indicating that electrostatic interactions are partially involved in the binding of CRAMP (16–33) to FtsZ. KCl (250 mM) did not significantly influence the assembly kinetics of FtsZ (Figure S3A of the Supporting Information). Further, KCl (250 mM) affected neither the tryptophan fluorescence (Figure S3B of the Supporting Information) of mutated FtsZ (Y273W) nor the binding of ANS to FtsZ, indicating that it does not grossly alter the conformation of FtsZ (Figure S3C of the Supporting Information). However, it is possible that a high salt concentration can subtly alter the conformation of either FtsZ or the peptide. Preincubation of FtsZ with 100 and 150 μ M CRAMP (16–33) increased the fluorescence intensity of ANS by 34 ± 4 and $58 \pm 12\%$, respectively, compared to the control, indicating that CRAMP (16–33) induced conformational changes in FtsZ (Figure 2E). Consistent with the previous study,¹⁴ FtsZ was found to contain a high level of α -helical structures as evidenced by the presence of a single peak near 1653 cm^{-1} . The peptide showed mostly random coil structure as indicated by the presence of a single peak near 1640 cm^{-1} .

When FtsZ was incubated with 100 and 150 μ M CRAMP (16–33), two distinct peaks were observed in the amide I region of the FTIR spectra. The peak near 1653 cm^{-1} corresponds to the α -helical conformation and the peak near 1672 cm^{-1} to the β -turn structure (Figure 2F). The result suggested that CRAMP (16–33) altered the secondary structure of FtsZ.

The effect of CRAMP (16–33) on membrane integrity was monitored using a Live/dead Bac Light Bacterial Viability Kit (Molecular Probes).¹² *B. subtilis* cells were grown in the absence and presence of 20 μ M CRAMP (16–33) and stained with SYTO-9 and PI. The green fluorescence intensity was found to be 478 ± 97 and 481 ± 93 in the control and treated cells, respectively. When *B. subtilis* cells were grown in the presence of vancomycin, which is known to damage the bacterial membrane, the green fluorescence intensity was found to be reduced by $90 \pm 2\%$ compared to that of control cells (Figure S4A of the Supporting Information) and there was also a peak shift in the red region. Further, when the *B. subtilis* cells were grown without and with 20 μ M CRAMP (16–33) and stained with PI, the red fluorescence intensity was found to be 119 ± 16 and 116 ± 15 , respectively. When *B. subtilis* cells were grown in the presence of vancomycin, the red fluorescence intensity increased by 2-fold as compared to that of control cells (237 ± 30) (Figure S4B of the Supporting Information). These results suggested that 20 μ M CRAMP (16–33) did not perturb the membrane integrity of *B. subtilis* cells. A proper membrane potential is required for the localization of many proteins.¹⁵ The Z-ring-associated proteins FtsA, MinD, and MreB are ATPases, and a perturbation of the membrane potential can hamper the localization of these proteins.¹⁵ *B. subtilis* cells were grown without and with 20 μ M CRAMP (16–33) and stained with 12 μ M 3,3'-diethyloxa-carbocyanine iodide (DiOC₂) (Bac Light Bacterial Membrane Potential Kit

from Molecular Probes).^{15–17} DiOC₂ emits red fluorescence in the monomeric form, but upon self-association, its emission maxima shift to green.¹⁸ An altered membrane potential is known to accumulate DiOC₂ molecules inside the cells, which produces green fluorescence.¹⁸ The green fluorescence intensity of DiOC₂ was 121 ± 8 and 119 ± 4 in the absence and the presence of 20 μ M CRAMP (16–33), respectively, indicating that the peptide did not affect the membrane potential of *B. subtilis* cells (Figure S4C of the Supporting Information). In case of CCCP (0.2 μ M), a known membrane potential inhibitor, the green fluorescence intensity was increased by $290 \pm 35\%$ compared to that of the control. Human RBC releases heme when membranes rupture, and heme displays absorbance at 405 nm.¹⁹ When RBC was incubated without and with 20 and 30 μ M CRAMP (16–33), the absorbance of the heme group at 405 nm was found to be similar in the control and treated samples, whereas the absorbance was increased by $290 \pm 35\%$ in the sample treated with saponin (0.02%) (Figure S5 of the Supporting Information). The result suggested that CRAMP (16–33) treatment did not lyse the RBC membrane.

Antibacterial Mechanism of Action of CRAMP (16–33). CRAMP (16–33) bound to FtsZ *in vitro* and inhibited the assembly and GTPase activity of purified FtsZ. *In silico* analysis of the binding of CRAMP (16–33) to FtsZ revealed that it binds to FtsZ in the C-terminal domain adjacent to the T7 loop. It has been reported that when GTP binds to a monomeric FtsZ, the T7 loop protrudes out from the FtsZ monomer and interacts with another FtsZ monomer.^{13,20,21} The T7 loop of FtsZ plays an essential role in the assembly of adjacent FtsZ monomers.²⁰ CRAMP (16–33) interacts with the T7 loop of FtsZ, which may perturb the association between FtsZ monomers and thereby reduces the GTPase activity of FtsZ. A molecular docking study indicated that Lys25 of CRAMP (16–33) and Asp287 of FtsZ form a salt bridge. The polymerization inhibitory effect of CRAMP (16–33) was found to be reduced in the presence of salt, indicating that the ionic interactions are partially responsible for the binding of CRAMP (16–33) and FtsZ. CRAMP (16–33) enhanced the fluorescence intensity of the ANS-FtsZ complex, indicating that the binding of CRAMP (16–33) induces conformational changes in FtsZ. Further, the FTIR data indicated that CRAMP (16–33) also perturbed the secondary structure of FtsZ. CRAMP (16–33) induced elongation of *B. subtilis* cells and perturbed Z-ring formation in these cells. However, CRAMP (16–33) appeared to perturb neither the membrane integrity nor the membrane potential of *B. subtilis* cells. The results suggested that CRAMP (16–33) stalled bacterial cytokinesis by inhibiting FtsZ assembly. The concentration of CRAMP (16–33) required to inhibit the proliferation of *B. subtilis* cells was found to be several-fold lower than that required to inhibit the assembly of FtsZ *in vitro*. A partial inhibition of the assembly of FtsZ may inhibit Z-ring formation in bacteria and thereby stalls the bacterial division process. It is also possible that CRAMP (16–33) accumulates inside the cells, and the intracellular concentration of CRAMP (16–33) in bacteria may be significantly higher than that of the media. Interestingly, CRAMP (16–33) (100 μ M) did not affect the proliferation of human small cell lung cancer (SCLC) cells in culture.⁷ CRAMP (16–33) also did not lyse the membrane of human RBC, indicating that CRAMP (16–33) preferentially acts on the bacterial cells and suggested that it may have therapeutic potential against bacterial infection.

■ ASSOCIATED CONTENT

■ Supporting Information

Description of experimental procedures, figures, and tables. This material is available free of charge via the Internet at <http://pubs.acs.org>.

■ AUTHOR INFORMATION

Corresponding Author

*E-mail: panda@iitb.ac.in. Phone: +912225767838.

Funding

The work is supported by a grant from the Department of Science and Technology, Government of India, to D.P.

Notes

The authors declare no competing financial interest.

■ ACKNOWLEDGMENTS

We sincerely thank Dr. L. W. Hamoen (Newcastle University, Newcastle upon Tyne, U.K.) for providing GFP clones. We thank Dr. Ankit Rai and Dr. Anusri Bhattacharyya for critical reading of the manuscript.

■ REFERENCES

- (1) Bergman, P., Johansson, L., Wan, H., Jones, A., Gallo, R. L., Gudmundur, G. H., Hokfelt, T., Jonsson, A. B., and Agerberth, B. (2006) Induction of the antimicrobial peptide CRAMP in the blood-brain barrier and meninges after meningococcal infection. *Infect. Immun.* 74, 6982–6991.
- (2) Wiesner, J., and Vilcinskas, A. (2010) Antimicrobial peptides the ancient arm of the human immune system. *Virulence* 1, 440–464.
- (3) Gallo, R. L., Kim, K. J., Bernfield, M., Kozaki, C. A., Zanetti, M., Merluzzi, L., and Gennaro, R. (1997) Identification of CRAMP, a cathelin-related antimicrobial peptide expressed in the embryonic and adult mouse. *J. Biol. Chem.* 272, 13088–13093.
- (4) Chromek, M., Arvidsson, I., and Karpman, D. (2012) The antimicrobial peptide cathelicidin protects mice from *Escherichia coli* O157:H7-mediated disease. *PLoS One* 7, e46476.
- (5) Rosenberger, C. M., Gallo, R. L., and Finlay, B. B. (2004) Interplay between antibacterial effectors: A macrophage antimicrobial peptide impairs intracellular *Salmonella* replication. *Proc. Natl. Acad. Sci. U.S.A.* 101, 2422–2427.
- (6) Ryan, L., Lamarre, B., Diu, T., Ravi, J., Judge, P. J., Temple, A., Carr, M., Cerasoli, E., Su, B., Jenkinson, H. F., Martyna, G., Crain, J., Watts, A., and Ryadnov, M. G. (2013) Anti-antimicrobial peptides: folding-mediated host defense antagonists. *J. Biol. Chem.* 288, 20162–20172.
- (7) Ha, J.-M., Shin, S. Y., and Shin, S. W. (1999) Synthesis and antibiotic activities of CRAMP, a cathelin-related antimicrobial peptide and its fragments. *Bull. Korean Chem. Soc.* 20, 1073–1077.
- (8) Handler, A. A., Lim, J. E., and Losick, R. (2008) Peptide inhibitor of cytokinesis during sporulation in *Bacillus subtilis*. *Mol. Microbiol.* 68, 588–599.
- (9) Lock, R. L., and Harry, E. J. (2008) Cell-division inhibitors: new insights for future antibiotics. *Nat. Rev. Drug Discovery* 7, 324–338.
- (10) Kapoor, S., and Panda, D. (2009) Targeting FtsZ for antibacterial therapy: a promising avenue. *Expert Opin. Ther. Targets* 13, 1037–1051.
- (11) Gamba, P., Veening, J. W., Saunders, N. J., Hamoen, L. W., and Daniel, R. A. (2009) Two-step assembly dynamics of the *Bacillus subtilis* divisome. *J. Bacteriol.* 191, 4186–4194.
- (12) Singh, P., Jindal, B., Surolia, A., and Panda, D. (2012) A rhodanine derivative CCR-11 inhibits bacterial proliferation by inhibiting the assembly and GTPase activity of FtsZ. *Biochemistry* 51, 5434–5442.
- (13) Ray, S., Kumar, A., and Panda, D. (2013) GTP regulates the interaction between MciZ and FtsZ: a possible role of MciZ in bacterial cell division. *Biochemistry* 52, 392–401.

- (14) Shin, J. Y., Vollmer, W., Lagos, R., and Monasterio, O. (2013) Glutamate 83 and arginine 85 of helix H3 bend are key residues for FtsZ polymerization, GTPase activity and cellular viability of *Escherichia coli*: lateral mutations affect FtsZ polymerization and *E. coli* viability. *BMC Microbiol.* 13, 13–26.
- (15) Strahl, H., and Hamoen, L. W. (2010) Membrane potential is important for bacterial cell division. *Proc. Natl. Acad. Sci. U.S.A.* 107, 12281–12286.
- (16) Laflamme, C., Lavigne, S., Ho, J., and Duchaine, C. (2004) Assessment of bacterial endospore viability with fluorescent dyes. *J. Appl. Microbiol.* 96, 684–692.
- (17) Shapiro, H. M. (2000) Membrane potential estimation by flow cytometry. *Methods* 21, 271–279.
- (18) Foss, M. H., Eun, Y. J., Grove, C. I., Pauw, D. A., Sorto, N. A., Rensvold, J. W., Pagliarini, D. J., Shaw, J. T., and Weibel, D. B. (2013) Inhibitors of bacterial tubulin target bacterial membranes *in vivo*. *Med. Chem. Commun.* 4, 112–119.
- (19) Eun, Y. J., Foss, M. H., Kiekebusch, D., Pauw, D. A., Westler, W. M., Thanbichler, M., and Weibel, D. B. (2012) DCAP: a broad-spectrum antibiotic that targets the cytoplasmic membrane of bacteria. *J. Am. Chem. Soc.* 134, 11322–11325.
- (20) Oliva, M. A., Cordell, S. C., and Löwe, J. (2004) Structural insights into FtsZ protofilament formation. *Nat. Struct. Mol. Biol.* 11, 1243–1250.
- (21) Huecas, S., Schaffner-Barbero, C., García, W., Yébenes, H., Palacios, J. M., Díaz, J. F., Menéndez, M., and Andreu, J. M. (2007) The interactions of cell division protein FtsZ with guanine nucleotides. *J. Biol. Chem.* 282, 37515–37528.